2000

EGO-1 is related to RNA-directed RNA polymerase and functions in germ-line development and RNA interference in C. elegans

Anne Smardon
Axys Pharmaceuticals, NemaPharm Division

Jill M. Spoerke
Axys Pharmaceuticals, NemaPharm Division

Steven C. Stacey
University at Buffalo School of Dental Medicine

Marcia E. Klein
University of Medicine and Dentistry of New Jersey, New Jersey Medical School

Nancy Mackin
Syracuse University

See next page for additional authors

EGO-1 is related to RNA-directed RNA polymerase and functions in germ-line development and RNA interference in *C. elegans*

Anne Smardon*, Jill M. Spoerke*†, Steven C. Stacey‡, Marcia E. Klein§, Nancy Mackin¶ and Eleanor M. Maine¶

Background: Cell-fate determination requires that cells choose between alternative developmental pathways. For example, germ cells in the nematode worm *Caenorhabditis elegans* choose between mitotic and meiotic division, and between oogenesis and spermatogenesis. Germ-line mitosis depends on a somatic signal that is mediated by a Notch-type signaling pathway. The *ego-1* gene was originally identified on the basis of genetic interactions with the receptor in this pathway and was also shown to be required for oogenesis. Here, we provide more insight into the role of *ego-1* in germ-line development.

Results: We have determined the *ego-1* gene structure and the molecular basis of *ego-1* alleles. Putative *ego-1* null mutants had multiple, previously unreported defects in germ-line development. The *ego-1* transcript was found predominantly in the germ line. The predicted EGO-1 protein was found to be related to the tomato RNA-directed RNA polymerase (RdRP) and to *Neurospora crassa* QDE-1, two proteins implicated in post-transcriptional gene silencing (PTGS). For a number of germ-line-expressed genes, *ego-1* mutants were resistant to a form of PTGS called RNA interference.

Conclusions: The *ego-1* gene is the first example of a gene encoding an RdRP-related protein with an essential developmental function. The *ego-1* gene is also required for a robust response to RNA interference by certain genes. Hence, a protein required for germ-line development in *C. elegans* may be a component of the RNA interference/PTGS machinery.

Address: ¶Department of Biology, Syracuse University, 108 College Place, Syracuse, New York 13244, USA.

Present addresses: †Axys Pharmaceuticals, NemaPharm Division, 180 Kimball Way, South San Francisco, California 94080, USA. ‡University at Buffalo School of Dental Medicine, Buffalo, New York 14214, USA. §University of Medicine and Dentistry of New Jersey, New Jersey Medical School, 185 South Orange Avenue, University Heights, Newark, New Jersey 07103, USA.

*A.S. and J.M.S. contributed equally to this work.

Correspondence: Eleanor M. Maine
E-mail: emmaine@syr.edu

Received: **4 October 1999**
Revised: **25 November 1999**
Accepted: **7 December 1999**

Published: **3 February 2000**

Current Biology 2000, 10:169–178

0960-9822/00/$ – see front matter

Background

Germ-line development in *Caenorhabditis elegans* requires the coordinate regulation of cell proliferation, sex determination, meiotic progression and gamete formation [1]. These diverse processes are regulated in a variety of ways, as illustrated by three brief examples. Proliferation depends on an inductive signal from somatic distal-tip cells that is mediated by a Notch-type signaling pathway (see [2,3]). Sex determination relies on a genetic pathway that specifies differentiation of sperm in males and larval hermaphrodites, and then is reset to specify oogenesis in the adult hermaphrodite [4]. Entry into meiosis (and, consequently, gametogenesis) depends on the activity of two redundant pathways, mediated by GLD-1 and GLD-2 proteins [5–7].

Weak alleles of *ego-1* were originally identified in screens for mutations that interact genetically with the inductive pathway that signals germ-line proliferation [8]. These alleles disrupt oogenesis and cause sterility. In studies reported here, we recovered and characterized *ego-1* null alleles, and found that they disrupted germ-line development in multiple ways. Defects occurred in gametogenesis, proliferation and meiosis; of these, only abnormal oogenesis has previously been associated with *ego-1* [8]. Consistent with its germ-line-specific phenotype, we found the *ego-1* transcript primarily (if not entirely) in the germ line.

The predicted EGO-1 protein is related to tomato RNA-directed RNA polymerase (RdRP) [9] and *Neurospora crassa* QDE-1 protein [10]. The *qde-1* gene was identified in screens for mutants defective in a post-transcriptional gene silencing (PTGS) phenomenon called quelling [11]. Similar phenomena, often called co-suppression, have been described in plant species (see [12]). They are related in many respects to RNA-mediated genetic silencing (also called RNA interference or RNAi) in *C. elegans* (see [13,14]). RdRP is also suspected to function in PTGS (see Discussion). One implication of the homology between EGO-1, QDE-1 and RdRP is that *ego-1* might function in PTGS in *C. elegans*. We found that *ego-1* mutants were indeed insensitive or weakly sensitive to RNAi in the expression of some, but not all, germ-line-expressed genes. We also found that some *ego-1* mutations disrupted the RdRP/QDE-1-conserved region, implicating this domain in EGO-1 function. Hence, *ego-1* is a gene with an essential role in germ-line development and encodes what appears to be a component of the RNAi machinery.

Table 1

Time course of germ-line development in *ego-1* mutants.

	Age at first appearance of a given nuclear morphology				
Genotype	Transition nuclei	Pachytene nuclei	Abnormal distal nuclei	Primary spermatocytes	Oocyte nuclei
unc-29	40 h	44 h	–	52 h	60 h
om58 unc-29	36 h	40 h	44 h	48 h	64 h
om18 unc-29	36 h	40 h	40 h	52 h	60 h
om54 unc-29; om97 unc-29	36 h	40 h	nd	nd	nd
unc-32	36 h	40 h	nd	nd	nd
om58 unc-32	32 h	40 h	nd	nd	nd
Wild type (N2)	36 h	40 h	–	48 h	56 h

The table shows the earliest time point at which a given nuclear morphology was seen in any of the gonad arms that was scored (h, hours post-hatching; nd, not determined; $n \geq 20$ gonad arms except for *ego-1;unc-32* where $n = 12$ at 40 h). In general, ≥ 50% of the scored arms contained the nuclei in question, but only 5% of *unc-29* gonad arms contained transition nuclei at 40 h ($n = 38$). Previously, we reported that meiosis was delayed briefly in *ego-1(om18)* mutants [8]. At that time, however, the effect of *unc-29* on germ-line development was not appreciated. Here, comparison of *unc-29* and N2 animals revealed that transition nuclei appeared 4 h later in *unc-29* mutants than they did in the wild type. Thus, the delayed germ-line development in *unc-29* mutants was suppressed by *ego-1*, and the onset of meiosis was earlier in *ego-1* animals that are not marked with *unc-29*. See Materials and methods.

Results

Two *ego-1* alleles (*om18*, *om71*) were previously reported as disrupting oogenesis and interacting with the Notch-type signaling pathway that promotes germ-line proliferation in *C. elegans* [8]. We isolated and characterized several additional alleles in order to determine the *ego-1* null phenotype (see Materials and methods). Dosage studies confirmed that the new alleles were recessive and likely to be associated with a loss of gene function. Comparison of *ego-1(–/–)* and *ego-1(–/Df)* animals (where *Df* indicates a chromosomal deficiency) showed that they had qualitatively similar phenotypes (compare panels c–e in Figure 1); development was normal in *ego-1*(–/–);*Dp[ego-1(+)]* germ lines, indicating that one dose of *ego-1(+)* rescues the *ego-1(–)* phenotype (see Materials and methods). The *om58*, *om84* and *om97* phenotypes were more severe than those of other alleles (see below). Molecular studies predicted that these three alleles produce truncated products, whereas the protein encoded by other alleles is of wild-type length (see below). Thus, *om58*, *om84* and *om97* are likely to be null for *ego-1* function.

Developmental defects in *ego-1* mutants

Severe *ego-1* mutants have multiple germ-line defects. Somatic development appears to be normal. To describe the *ego-1* phenotype in detail, the time course of germ-line development was examined using *om58* and *om18*, which are representative severe and weak alleles, respectively. Other alleles were examined at landmark time points. Germ-line development in *unc-29(e193)* animals served as a control as *unc-29* was used as a marker to identify *ego-1* homozygotes. The *unc-29* animals resembled the wild type (N2) except that the onset of meiotic prophase and subsequent gametogenesis were delayed by ~4 hours (Table 1, Figure 1a,b and data not shown). Germ-line defects in *ego-1* mutants are described below. Chromosome morphology was visualized using the dye 4,6-diamidino-2-phenylindole (DAPI; see Materials and methods).

Alterations in gametogenesis

The spermatogenesis-to-oogenesis switch occurred several hours later in *ego-1* mutants than in controls (Table 1 and data not shown). The *unc-29* animals had completed spermatogenesis and produced oocytes and some embryos by 58–60 hours. In contrast, spermatogenesis continued in most *ego-1(om58)* animals for another ~8 hours (66–68 hours). A similar effect was seen with all other alleles (Table 1 and data not shown). As a result of prolonged spermatogenesis, *om58* animals produced more sperm than did controls. For example, at 66–68 hours, *unc-29* controls had 106 ± 4 sperm and *om58 unc-29* mutants had 121 ± 6 sperm; when a one-way analysis of variance was used to test the difference in sperm count between control and *om58* animals, it was found to be significant ($p < 0.045$) [15].

In addition to being delayed, the switch from spermatogenesis to oogenesis appeared defective in *ego-1* hermaphrodites; mutants made morphologically normal sperm, but then typically produced small cells with unusual chromosome morphology before making recognizable oocytes (Figure 1c,e). This phenotype was observed with all alleles except *om18* and *om71*. These intermediate-sized germ cells could be abnormal primary spermatocytes or intersexual cells. In the latter case, they should form only in a germ line that switches sex from male to female. To test this idea, we used *fog-3* (for 'feminization of the

germ line'; [16]) and *mog-1* (for 'masculinization of the germ line'; [17]) mutations to feminize or masculinize the XX germ line, respectively, and then looked for production of intermediate cells. The *ego-1 fog-3* XX animals produced abnormal oocytes similar to those found in *ego-1* single mutants, but no intermediate germ cells were observed ($n = 64$ gonad arms). The *ego-1;mog-1* XX animals, like *ego-1* XO males, produced sperm but no intermediate germ cells ($n > 100$). Hence, intermediate cells were only observed when the germ line switched from spermatogenesis to oogenesis.

The *ego-1(–)* oocytes were small and could not support embryonic development (Figure 1c; see [8]); this phenotype has been described as Oog (for 'oogenesis defective') [8]. Oocyte nuclei often did not have the typical diakinesis morphology but, instead, some homologous chromosomes appeared unpaired (data not shown). This effect was observed for all alleles except *om18*, and was seen in *ego-1(om18/Df)* animals. The *ego-1* oocytes could be fertilized and produced an eggshell, but typically arrested as a loose ball of 20–50 cells without undergoing morphogenesis or forming muscle or gut cells (data not shown). When viewed under the dissecting microscope, *ego-1* adults initially appeared sterile because oogenesis was delayed, and then because the small oocytes were slow to be ovulated and fertilized. Ovulation occurred earlier in *om18*, *om54* and *om96* adults than in other *ego-1* mutants, and embryos frequently became visible in the uterus. Therefore, these three alleles produce a milder 'dissecting-microscope phenotype'.

Figure 1

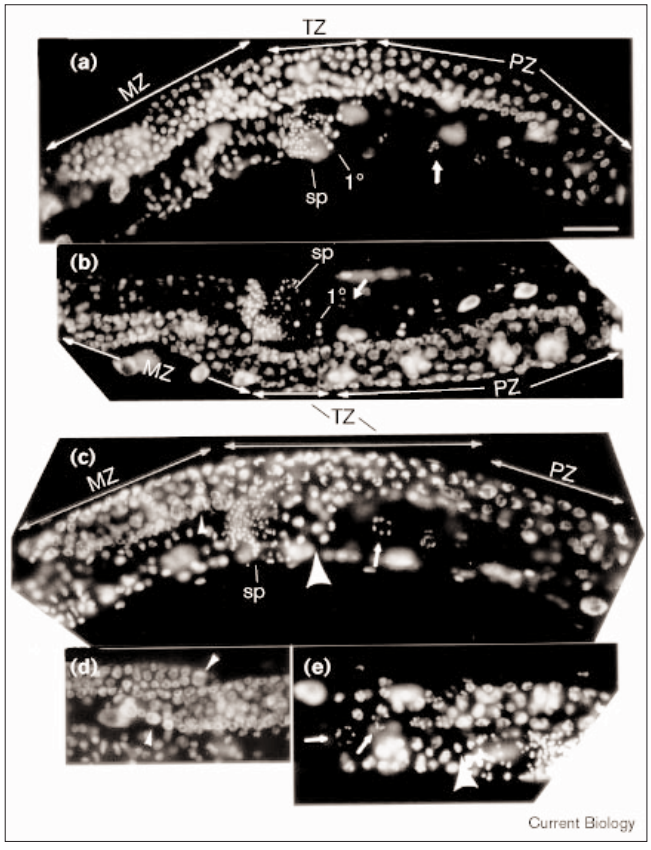

Germ-line defects in *ego-1* hermaphrodites. Chromosome morphology was visualized using DAPI. MZ, mitotic zone; TZ, transition zone; PZ, pachytene zone; small arrowheads, abnormal distal nuclei; small arrows, oocyte nucleus in diakinesis; large arrowheads, 'intermediate' nuclei; 1°, primary spermatocytes; sp, sperm (see text). **(a)** Wild-type (N2) adult germ line. **(b)** The *unc-29* control germ line. **(c)** Enlarged TZ and intermediate nuclei in an *ego-1(om97)* mutant. **(d)** Abnormal distal nuclei in an *ego-1(om97)* mutant. **(e)** Slightly higher magnification view of intermediate cells in an *ego-1(om58/ozDf5)* mutant. See text and Figure 2 for details. The scale bar represents 10 mm; (a–d) are printed to the same scale. The embryos in (c–e) are marked with the *unc-29* mutation.

Alterations in mitosis and meiosis

Young *ego-1* mutants contained three other defects, which are described here in order of appearance. The first sign of meiosis in wild-type *C. elegans* is the presence of nuclei in very early meiotic prophase; they are morphologically distinct from mitotic nuclei and from meiotic nuclei that have progressed on to the pachytene stage (Figure 1a–c). These early meiotic nuclei are referred to as being in 'transition' from mitosis to the pachytene stage (see [5]). In *ego-1* animals, transition nuclei were visible several hours earlier than in controls: they were present in most *ego-1 unc-29* mutant germ lines at 34–36 hours but not in *unc-29* control animals until several hours later (42–44 hours; Table 1). Similarly, ~1–2 transition nuclei were present in some *ego-1;unc-32* gonad arms (50%) at 30–32 hours whereas they were not present in *unc-32* controls until 34–36 hours (68%). (The remaining animals had no transition nuclei yet.) In contrast, by 34–36 hours, 100% of *ego-1;unc-32* animals contained several transition nuclei ($n = 18$ arms).

The *ego-1* mutants had large, diffusely staining nuclei in the distal arm of the gonad that were not found in the wild type or in *unc-29* controls (Figure 1c,d). The number of such nuclei per animal averaged from 1 ± 1 to 6 ± 2, depending on the allele or heteroallelic combination examined. In time-course experiments, abnormal nuclei were first visible at early/mid-L4 stage (40–44 h; Table 1) and became more numerous in older animals.

In *ego-1* mutants, the region containing transition nuclei (the 'transition zone', or TZ) appeared enlarged and the pachytene zone (PZ) reduced relative to the wild type (Figure 1a–c). This effect was quantified by determining the size of individual mitotic, transition and pachytene zones relative to the entire distal germ line (see Materials and methods). Data were normalized for differences in total germ cell numbers in different genetic backgrounds. In *unc-29* controls, the mitotic zone (MZ), TZ, and PZ comprised 35%, 8% and 57%, respectively, of the distal germ line; this distribution resembles the wild type

Figure 2

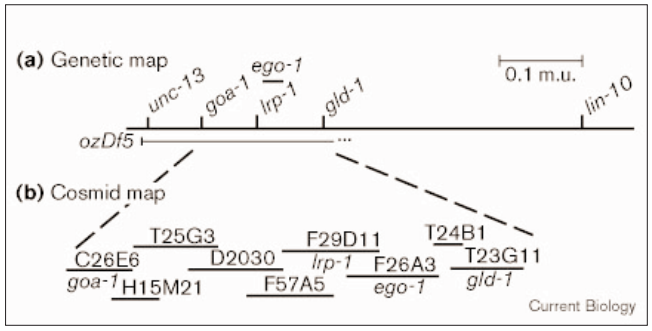

Genetic and physical map position of *ego-1*. **(a)** The *ego-1* gene maps between *goa-1* and *gld-1*, very close or to the right of *lrp-1*; it is uncovered by the deficiency *ozDf5* (see Materials and methods; m.u., map units). **(b)** The relative position of each cosmid used to locate *ego-1* is indicated; those cosmids containing *ego-1, goa-1, lrp-1* and *gld-1* are indicated.

Figure 3

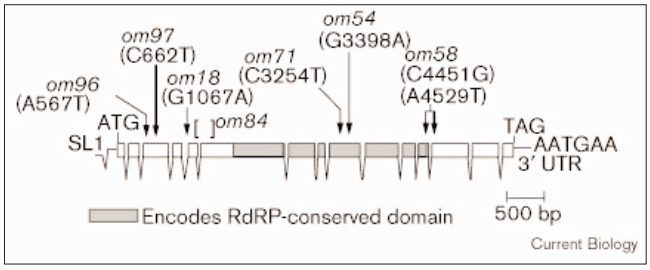

The *ego-1* gene structure and mutant lesions. The *ego-1* message contains 15 exons (boxes) and an SL1 *trans*-spliced leader. Arrows indicate the position of mutant lesions; square brackets denote the region of the RNA that is deleted in the *om84* mutation; mutations that produce a stop codon are indicated by the square brackets or bold arrows. Nucleotide changes are indicated in parentheses. UTR, untranslated region. In *om84*, nucleotides 1106–1357 are deleted and a T is inserted at nucleotide 1107. Sequence changes produce the following results: *om18*, 3′ splice acceptor changed, intron 4; *om54*, Glu979→Lys; *om58*, Cys1276→Trp, Lys1287→Stop (UAG); *om71*, Pro931→Ser; *om84*, Asn346→Stop (UAA); *om96*, His139→Leu; *om97*, Gln171→Stop (UAA). The *ego-1* cDNA sequence has been deposited in GenBank (accession number AF159143).

(see [5]). In *ego-1* mutants, the TZ was enlarged 2.5–4.5-fold relative to controls depending on the allele examined, and the PZ was reduced. For example, in *ego-1(om58)* adults, the MZ, TZ and PZ comprised 40%, 32% and 28% of the distal germ line, respectively. Thus, at any given time, *ego-1* germ lines contain a larger proportion of transition nuclei than do control germ lines.

The *ego-1* phenotype in males

Germ-line defects in *ego-1* males included a reduced number of germ cells, enlarged TZ, and abnormal distal nuclei as found in hermaphrodites (Table 1 and data not shown). These results are consistent with the ability of *ego-1* mutations to enhance the phenotype of *glp-1* mutations in both sexes ([8]; this study) and may indicate that *ego-1* has a common function(s) in male and hermaphrodite germ lines.

To test whether *ego-1* mutants make functional sperm, *ego-1 unc-29* males were mated to *unc-13* hermaphrodites and to *fem-1* (for 'feminization of the germ line') or *fog-1* XX animals that do not produce their own sperm. Cross progeny were not detected in any case. (In equivalent control crosses, *ego-1(+) unc-29* males produced numerous progeny.) When examined, the *fem* or *fog* animals contained sperm that must have been transferred by the *ego-1* males. Therefore, male *ego-1* sperm are apparently incapable of fertilization despite their normal appearance under differential interference contrast (DIC) optics and upon DAPI staining.

The *ego-1* gene structure

Genetic mapping placed *ego-1* between *goa-1* and *gld-1* (Figure 2a; see Materials and methods). Genomic DNA from seven *ego-1* mutants was probed for restriction fragment length polymorphisms using cosmids spanning the *goa-1* to *gld-1* region (Figure 2b). One cosmid, F26A3, detected a small deletion in the ultraviolet radiation (UV)-induced mutant *ego-1(om84)* (Figures 2,3). DNA from the vicinity of the *ego-1(om84)* deletion, when used to probe blots of total worm RNA from mixed-stage wild-type animals, detected an ~5.5 kb transcript (Figure 4). Reverse transcription (RT)–PCR products and cDNAs corresponding to the entire transcript were then isolated and fully sequenced (see Materials and methods). The *ego-1* gene structure is schematically illustrated in Figure 3; *ego-1* corresponds to roughly the 5′ half of a predicted gene designated F26A3.3 by the *C. elegans* sequencing consortium [18]. Sequence data revealed an open reading frame of 4896 nucleotides that is predicted to encode a 1632 amino-acid protein (Figure 5 and see Supplementary material).

The predicted EGO-1 protein is related to proteins implicated in PTGS

EGO-1 belongs to a protein family containing tomato RdRP (GenBank accession number Y10403) [9] and *N. crassa* QDE-1 (GenBank accession number AJ133528) [10,11]. Homology was higher between EGO-1 and tomato RdRP than between EGO-1 and QDE-1, but both homologies were significant (expected values of 7×10^{-78} and 8×10^{-7}, respectively, using BLAST). EGO-1 is also related to RdRP family members of unknown function in *C. elegans* (see below), *Arabidopsis thaliana* (GenBank accession number AF080120, expected value 6×10^{-66}, and several others), *Schizosaccharomyces pombe* (GenBank accession number Z98533, expected value 10^{-59}) and *Phanerochaete chrysosporium* (GenBank accession number Z31373, expected value 4×10^{-17}). Figure 5 shows an

alignment of the most highly conserved region, overall, among representative RdRP family members.

Those proteins most closely related to EGO-1 are the products of three *C. elegans* genes: the immediate downstream gene (corresponding to the 3′ ~half of F26A3.3; GenBank accession number AF159144), M01G12.12 (GenBank accession number Z81571) and F10B5.7 (GenBank accession number Z48334). We renamed the *ego-1* paralogs *rrf-1*, *rrf-2* and *rrf-3*, respectively, for RdRP family. An alignment of the four proteins is shown in the Supplementary material. RRF-1 is predicted from the complete cDNA sequence (A.S. and E.M.M., unpublished data) and is ~58% identical overall to EGO-1. Both *ego-1* and *rrf-1* mRNAs are *trans*-spliced to SL1, and hence the two genes are distinct (that is, not members of a polycistron). RRF-2 and RRF-3 are predicted mainly from genomic DNA sequence and are 60% and 31% identical overall to EGO-1, respectively.

Figure 4

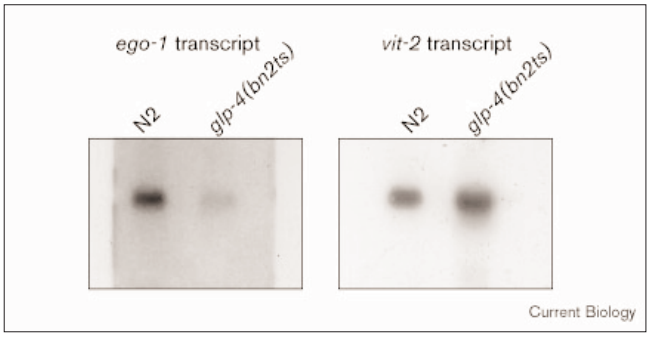

The *ego-1* transcript is highly germ-line enriched. RNA from wild-type (N2) worms and germ-line-deficient *glp-4(bn2ts)* mutants was compared. An *ego-1* probe detected a transcript of ~5.5 kb in total RNA from wild-type worms but not from *glp-4(bn2ts)* mutants. In contrast, the somatic *vit-2* (yolk-protein gene) transcript was detected at similar levels in both strains.

Molecular nature of *ego-1* mutations

The *ego-1* mutations were analyzed to identify null alleles and critical residues within the EGO-1 protein (Figure 3). DNA corresponding to *ego-1* was amplified from individual mutant animals and sequenced (see Materials and methods). The *om84* deletion introduces a stop codon in the reading frame; hence, *om84* is predicted to encode a severely truncated protein without activity. The *om97* allele was also found to contain a stop codon early in the coding region and is unlikely to have EGO-1 activity. The *om58* allele was found to have two lesions: it is predicted to encode a truncated product of 1287 amino acids with a missense mutation close to the carboxyl terminus. Because the *om58* open reading frame is relatively long (~79% of the full-length open reading frame) and contains the RdRP-related region, it may encode a product with some activity.

Four phenotypically weaker alleles were found to have point mutations that might cause a partial loss of gene function (Figure 3). The *om54*, *om71* and *om96* alleles have missense mutations in well-conserved residues; the *om54* and *om71* lesions are located within the RdRP-conserved domain (Figure 5). The *om18* allele contains an altered splice acceptor sequence in intron four. Examples of such mutations causing a partial loss of gene function have been described [19]; in these cases, splicing occurs at the proper site in a subset of transcripts.

Tissue specificity of the *ego-1* transcript

To determine whether the *ego-1* transcript is germ-line-specific, as might be predicted from the *ego-1* phenotype, we compared the transcript levels in wild-type worms and germ-line-deficient mutants (see Materials and methods). The conditional *glp-4(bn2ts)* mutation [20] was used to grow up a large population of animals with very small germ lines. In RNA prepared from *glp-4(bn2ts)* mutants grown at 25°C, *ego-1* transcripts were barely detectable (Figure 4), suggesting they are either specific to or highly enriched in the germ line. In contrast, the intestine-specific transcript from a yolk-protein gene, *vit-2*, was present at high levels in both strains (Figure 4). As *glp-4(bn2ts)* animals contain a few germ cells, the low level of *ego-1* transcript in these animals could be present in the soma and/or germ line.

The *ego-1* gene and RNAi

We tested whether *ego-1* functions in RNAi. Double-stranded RNA (dsRNA) corresponding to each of several genes was injected into *ego-1* mutants and their response monitored. Wild-type and *ego-1(+/–)* animals were injected in parallel to control for effectiveness of the procedure (see Materials and methods). We mainly tested germ-line-expressed genes, because *ego-1* is itself expressed predominantly in the germ line.

The *ego-1* mutants had approximately normal sensitivity to *unc-22* and *lag-1* dsRNAs, yet little or no sensitivity to *gld-1*, *mpk-1* and *ncc-1* dsRNAs (Table 2; see below). The *unc-22*-injected animals were scored for an uncoordinated 'Twitcher' phenotype [21]. The *lag-1*-injected animals were scored for loss of the distal mitotic zone [22]. Animals injected with *gld-1*, *mpk-1* or *ncc-1* were scored as described below. Interestingly, injection of dsRNA *per se* appeared to enhance the *ego-1* germ-line-defective phenotype when compared with uninjected *ego-1* animals of the same age (data not shown).

Injection of *mpk-1* dsRNA produced a severe pachytene-exit defect (Pex phenotype; [23]) in control animals within 2 days at 20°C, yet produced almost no response in *ego-1* mutants (Table 2). To confirm that *mpk-1* dsRNA was indeed transferred to *ego-1* animals during

Figure 5

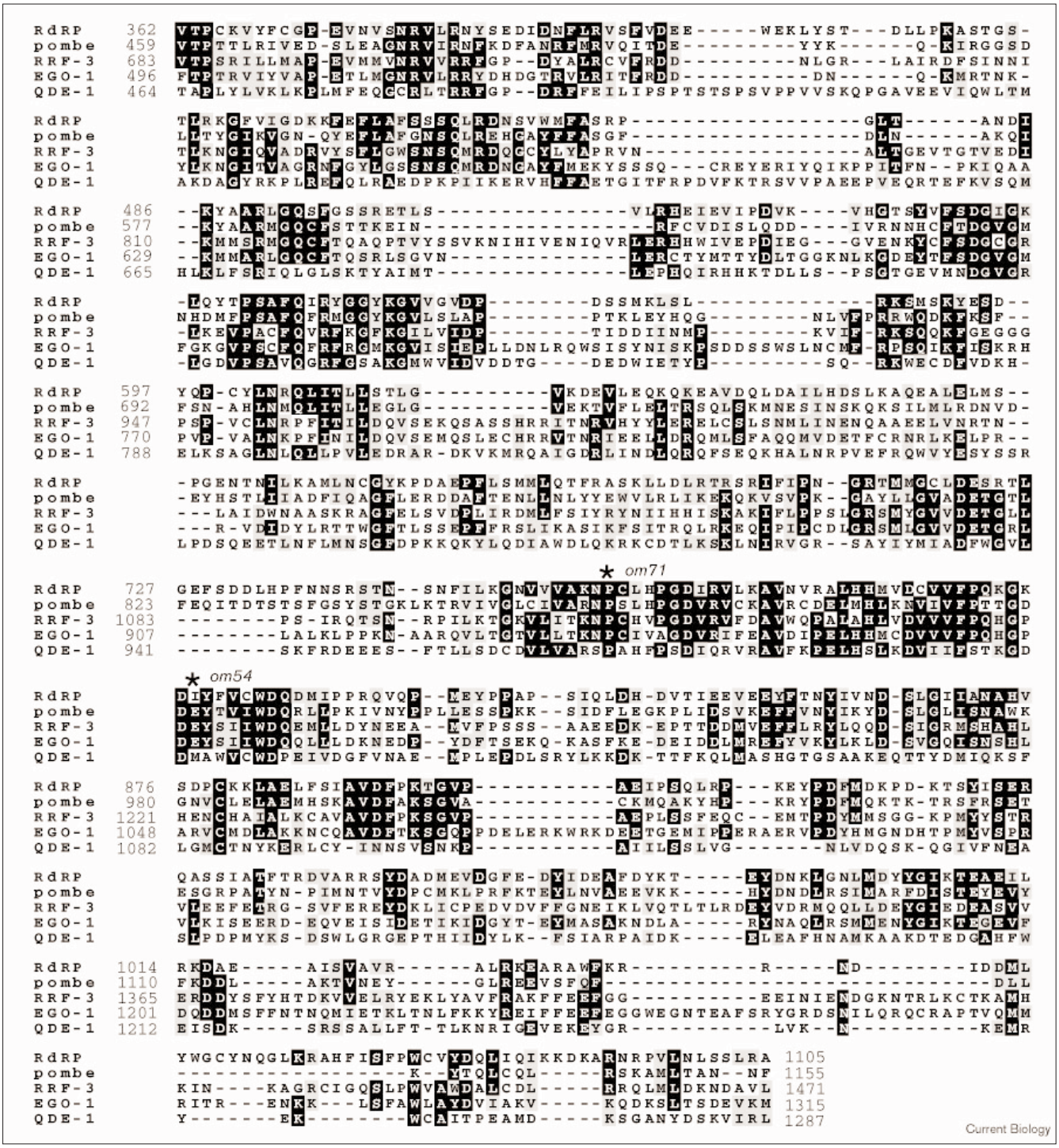

Amino-acid alignment of EGO-1 with predicted proteins from a variety of species: tomato RdRP; an *S. pombe* protein (pombe); *C. elegans* RRF-3; and *Neurospora* QDE-1. Only the region of conservation with EGO-1 is shown. Shaded residues are conserved in > 50% of the proteins; identical residues are shown on a black background and conservative substitutions are shown on gray. Locations of missense mutations are indicated by asterisks. See text.

the injections, *mpk-1* and *unc-22* dsRNAs were coinjected. After 3 days at 20°C, most injected animals (92% of controls, 100% of experimental animals) had an *unc-22* phenotype and 98% of controls had a severe Pex phenotype

Table 2

Tests for RNAi in an *ego-1* mutant background.

Gene(s) tested	Post-injection conditions	RNAi phenotype in control animals	RNAi phenotype in *ego-1(null)* animals
gld-1	3 days, 20°C	100% Proximal MZ ($n = 26$)	0% Proximal MZ ($n = 48$)
mpk-1	2 days, 20°C	100% Pex ($n = 58$)	3% Pex ($n = 36$)
unc-22 + *mpk-1*	3 days, 20°C	98% Pex ($n = 84$)	31% Pex ($n = 26$)
		92% Twitcher ($n = 53$)	100% Twitcher ($n = 13$)
unc-22	4 days, 20°C	87% Twitcher ($n = 15$)	82% Twitcher ($n = 22$)
ncc-1	2 days, 20°C	94% MZ absent ($n = 67$)	23% MZ absent ($n = 30$)*
lag-1	3 days, 20°C	78% MZ absent ($n = 68$)	67% MZ absent ($n = 18$)*

Injected animals were examined after 2–4 days as appropriate for the gene in question (see Materials and methods); *n*, number of gonad arms (germ-line phenotypes) or animals (*unc-22*) scored. Although most of the tested genes are pleiotropic, animals were scored for those defects clearly discernible in an *ego-1* mutant background, as follows: *unc-22*, animals twitch when paralyzed in levamisole (Twitcher); *gld-1*, mitotic nuclei are present proximal to the pachytene zone (Proximal MZ); *mpk-1*, meiotic nuclei fail to progress beyond pachytene stage and nuclei clump together (Pex); *lag-1* and *ncc-1*, germ-line mitosis ceases, leaving meiotic germ cells and/or gametes (MZ absent). For phenotypic details, see [5] for *gld-1*; [24] for *mpk-1*; [23] for *lag-1*; [21] for *unc-22* and [24] for *ncc-1*. *Values are corrected for the low level of MZ loss observed in uninjected *ego-1(null)* animals over the same time period; see Materials and methods.

(Table 2). In contrast, only 31% of *ego-1* gonad arms were mildly Pex and none were severely so. Thus, successful injection of *mpk-1* dsRNA into *ego-1* animals elicits only a very delayed, weak response. As a control, we examined *ego-1(null); mpk-1(null)* double mutants (see Materials and methods). These animals are Pex ($n = 20$ animals); hence, the failure of *ego-1(null);mpk-1(RNAi)* animals to become Pex does not reflect suppression by *ego-1(null)*.

Control animals injected with *gld-1* dsRNA became oogenesis-defective within 2 days and acquired a second, proximal mitotic zone (that formed a tumor) within 3 days (Table 2 and data not shown; see [5]). Because *ego-1* mutants also make defective oocytes, we scored injected *ego-1* animals for the proximal mitosis phenotype. After 3 days at 20°C, no injected *ego-1* animals contained a proximal mitotic zone although 100% of controls did so (Table 2). Therefore, *gld-1* appears to be resistant to RNAi in an *ego-1(null)* background. As a control, we wanted to examine whether *ego-1* suppresses *gld-1*. Because the two genes map very close together and are not flanked by suitable markers, we did not construct a double mutant; instead, we took advantage of the fact that injection of *ego-1* dsRNA produces a robust *ego-1(–)* phenotype in F1 animals. When *ego-1* was injected into *gld-2 gld-1 unc-29/hT2* animals, the *ego-1(RNAi)* phenotype did not suppress the *gld-2 gld-1* tumor [7]. Hence, *ego-1(null)* presumably does not suppress *gld-1(null)*.

Control animals responded strongly to *ncc-1* dsRNA: after 2 days at 20°C, 94% of gonad arms had lost the mitotic zone and distal germ cells had entered meiosis (Table 2; see [24]). Furthermore, the chromosome morphology of most full-sized oocytes did not appear as fully condensed as in wild-type diakinesis (data not shown). In our hands, standard diakinesis nuclei were rare in these animals. In contrast, fully 77% of injected *ego-1* gonad arms retained a mitotic zone and 100% of them contained multiple diakinesis nuclei; only 22% ($n = 36$) contained oocytes with the unusual nuclear morphology noted in controls. As a control, we examined *ego-1(null);ncc-1(ts)* double mutants (see Materials and methods). Germ-line mitosis ceased in these animals ($n = 24$ animals), as in *ncc-1(ts)* single mutants under the same conditions; hence, the failure to see loss of the mitotic zone in *ego-1(null);ncc-1(RNAi)* animals does not reflect suppression by *ego-1(null)*.

Effects on signaling from distal tip cell to the germ line

To better understand the role of *ego-1* in germ-line proliferation, we examined whether the loss of *ego-1* function enhances mutations in *lag-1*, a transcription factor activated by distal tip cell (DTC)-to-germ-line signaling [3]. We compared enhancement of *lag-1(om13ts)* [8] and *glp-1(bn18ts)* [25]. Our measure of DTC-to-germ-line signaling efficiency was the presence of mitotic germ cells. At 20°C, *lag-1(om13ts)* and *glp-1(bn18ts)* animals maintained a mitotic germ line throughout adulthood (this paper; [8]). At 12–24 hours after the adult molt, *ego-1* mutants typically contained mitotic germ cells, as well. In contrast, germ-line mitosis was generally absent from *ego-1;glp-1(ts)* animals by young adult stage or 12–24 hours later (depending on the *ego-1* allele) and from a significant percentage of *ego-1;lag-1(ts)* gonad arms in 12–24 hour-old adults (data not shown). In addition, germ cell counts indicated that *ego-1;glp-1* and *ego-1;lag-1* animals contained substantially fewer germ cells than did *ego-1*, *lag-1(ts)* or *glp-1(ts)* single mutants at the

same stage (data not shown). Hence, *ego-1* mutants, isolated as enhancers of *glp-1(ts)*, also enhance *lag-1(ts)*.

Discussion

The role of *ego-1* in germ-line development

The activity of the *ego-1* gene is critical for several aspects of cell proliferation and differentiation in the *C. elegans* germ line. The most obvious results of the loss of *ego-1* function are gametogenesis defects and subsequent sterility. In hermaphrodites, EGO-1 is required for the timely and clean transition from spermatogenesis to oogenesis and for the subsequent production of functional oocytes. EGO-1 may play a direct role in these events or influence them indirectly through its earlier function(s) in mitosis and/or meiotic prophase. There is precedence for the latter hypothesis in the analysis of *gld-1* gene activity. GLD-1 function is required for early meiotic progression in hermaphrodites, yet the lack of GLD-1 activity can result in abnormal oocytes later in development [5,6,26]. A similar requirement may exist for EGO-1 activity.

By mid-larval development, loss of *ego-1* function causes mitotic and meiotic defects. The earliest observed effect, premature meiosis, may reflect decreased efficacy of inductive signaling from DTC to germ line. Consistent with this hypothesis, *ego-1* mutations exacerbate the effects of decreased GLP-1 receptor and LAG-1 transcription factor activities. Also associated with the loss of *ego-1* function are abnormal nuclei in the distal germ line that appear arrested at an aberrant point in the cell cycle. This phenotype may reflect a role for EGO-1 in promoting germ-line mitosis *per se*. Once *ego-1* germ-line nuclei enter meiosis, they remain in early meiosis (presumably leptotene–zygotene) for longer than normal, perhaps because they have trouble executing an early step in meiotic prophase. A second meiotic defect is seen in full-grown oocytes where homologous chromosomes are unpaired. In yeast, failure to undergo meiotic recombination can result in desynapsis of chromosome pairs later in meiosis [27]. Unpaired homologs in *ego-1* oocytes may likewise reflect a recombination defect.

The role of *ego-1* in RNAi

EGO-1 is related to *N. crassa* QDE-1 and tomato RdRP, two proteins implicated in PTGS. The *qde-1* mutants are defective in quelling (PTGS) for each of several genes tested [11]. The connection between RdRP and PTGS is not as definitive, but quite plausible by the following logic. In general, PTGS phenomena are triggered by introduction of foreign DNA or RNA molecules, such as transgenes, RNA viruses and dsRNA (see [12–14]). PTGS is thought to be RNA-mediated (regardless of the initial trigger) and to require an RNA amplification step (see [14,21]). Tomato RdRP can transcribe RNA *in vitro* from RNA templates [9,28] and, if it has a similar *in vivo* activity, may amplify RNA during the PTGS response. A role for RdRP in PTGS is further substantiated by its sequence homology with QDE-1.

Given the similarity of EGO-1 to RdRP and QDE-1, we tested whether *ego-1* mutants are defective in RNAi, a form of PTGS that is well documented in *C. elegans* [21,29]. The *ego-1* mutants were largely resistant to RNAi in the expression of some germ-line genes. The one somatic gene tested was sensitive to RNAi, consistent with the germ-line expression of *ego-1*. Partial insensitivity to RNAi may be explained if EGO-1 is a component of the RNAi machinery whose function is partially redundant with that of another protein, such as one of the RRF proteins.

Does EGO-1 have separate roles in germ-line development and RNAi?

Mutations in *rde* (RNAi-deficient) and *mut* (mutator) genes have recently been reported that are strongly resistant to RNAi [30,31]. These mutants are fertile; therefore, at least some components of the RNAi machinery are not required for germ-line development. As *ego-1* is essential for germ-line development, its roles in development and RNAi may be different. Perhaps the biochemical function of EGO-1 is the same in both cases, but used to different advantage to regulate germ-line development and to promote RNAi. One possibility is that the developmental function of EGO-1 does not involve a PTGS mechanism of any kind. Alternatively, EGO-1 may function in a PTGS mechanism that regulates gene expression during development and is related, but not identical, to RNAi. In the latter case, the *ego-1* null phenotype might reflect a failure to downregulate gene expression at multiple points during germ-line development.

It is hypothesized that PTGS may be a critical defense against viral infection [14] and a means of limiting transposon density within the genome [31]. Our work shows that a gene with a developmental function encodes what appears to be a component of PTGS machinery. Further studies will investigate the relationship between EGO-1 function in development and in RNAi to determine whether PTGS is important in the regulation of development.

Conclusions

We have reported here that *ego-1* encodes a putative RdRP/QDE-1 family member whose activity is required for normal germ-line development in *C. elegans*. In the absence of *ego-1* activity, we observed reduced and, in some cases, defective germ-line mitosis, premature entry into meiosis, slow progression through early meiotic prophase, a delayed and incomplete switch from spermatogenesis to oogenesis, and production of abnormal oocytes. We have also shown that severe *ego-1* mutants have a gene-specific defect in dsRNA-mediated PTGS (RNAi). We identified several putative null alleles and have shown that the RdRP/QDE-1-conserved domain is required for EGO-1 activity. Finally, the *ego-1* transcript is present predominantly (if not entirely) in the germ line, suggesting that *ego-1* is transcribed in a tissue-specific manner.

Materials and methods

Culture conditions and strains

Standard culture conditions were used [32]. Wild-type strain *C. elegans* variant Bristol (N2) and mutant phenotypes are as described by Hodgkin [33] or as indicated. Nomenclature follows standard guidelines [33]. Mutations used were as follows. Linkage group (LG) I: *dpy-5* (*e61*), *ego-1* (*om18, om71*) [8], *fog-3* (*q443*) [16], *gld-1* (*q268, q485*) [5], *gld-2* (*dx32*) [7], *goa-1* (*n363*), *let-88* (*s132*), *lin-10* (*e1439*), *lrp-1* (*ku156*) (kindly supplied by J. Yochem), *unc-13* (*e1091*), *unc-29* (*e193*), *hT2* [34], *ozDf5* [5], *gaDp1* (kindly supplied by S. Kim); LGIII: *glp-1* (*bn18ts*) [25], *mog-1* (*q376*) [17], *mpk-1* (*ga117*) [35], *ncc-1* (*he25ts*) [24], *unc-32* (*e189*); LGIV: *lag-1* (*om13ts*) [8], *unc-5* (*e53*); LGV: *him-5* (*e1467ts*).

Isolation of ego-1 *mutations*

The *ego-1* mutations were isolated by a scheme described in Qiao *et al.* [8] following ethylmethane sulfonate (EMS) mutagenesis (*om54, om58, om96, om97*) or trimethylpsoralen/UV mutagenesis (*om84*). They map between *dpy-5* and *unc-29*, are uncovered by *ozDf5* (Figure 2 and data not shown), and fail to complement each other and two previously reported *ego-1* alleles, *om18* and *om71* [8]. Three-factor mapping of *om58, om71*, *om84*, and *om97* with *unc-13 let-88, unc-13 goa-1*, and *unc-13 lrp-1* placed them between *goa-1* and *gld-1*, very close or to the right of *lrp-1* (Figure 2 and data not shown).

Phenotypic characterization

Chromosome morphology was examined in animals fixed with −20°C methanol, stained with 0.5 μM DAPI, and mounted in Vectashield (Vector Labs). As a control, animals of several genotypes were dissected and fixed with 3% formaldehyde in 100 mM $KHPO_4$. Qualitatively similar results were obtained with each fixation method. To compare the relative sizes of the MZ, TZ and PZ, we chose one focal plane and counted the number of rows of nuclei in each zone. The TZ was defined as that region where at least two nuclei per row had the diagnostic 'crescent moon' morphology (see [5]). The portion of the total distal germ line represented by each zone was then calculated as the number of rows of nuclei within a given zone divided by the total number of rows in the three zones together; for example, number of rows in TZ / number of rows in (MZ + TZ + PZ). To examine the time course of germ-line development, synchronized animals were DAPI-stained and characterized as described [8]. The *ego-1(om58)* time points were taken every 4 h from 28 to 72 h; *ego-1(om18)* time points were taken every 4 h from 24 to 66 h. An *unc-29* time course was done in parallel as a control for each experiment. Staged *om54* and *om97* mutants were observed at landmark time points. Germ-line size was analyzed in young adult animals as described [8].

Stocks

The *ego-1(−)/ego-1(−0);ego-1(+)* animals were generated using *gaDp1*, a free duplication carrying *dpy-5(+)*, *ego-1(+)* and *unc-13(+)*. To generate *ego-1 fog-3* animals, we first constructed an *ego-1(om58) unc-29/unc-13 gld-1(q485) fog-3(q443)* stock; *fog* non-*unc* non-*gld* recombinants were isolated and tested for the presence of *ego-1* by crossing to *ego-1 unc-29/hT2* males. Balanced *ego-1 fog-3/hT2* animals were recovered from the same cross and used to maintain a stock. To generate *ego-1; mog-1* animals, we first crossed *ego-1 unc-29/hT2* males to *mog-1 unc-47/hT2* hermaphrodites. F1 males were then mated with *hT2* hermaphrodites. F2 non-*hT2* hermaphrodites were picked to individual plates to identify *ego-1 unc-29/hT2; mog-1 unc-47/hT2* individuals. Animals segregating *hT2* and sterile Unc-47 progeny were tested for the presence of *ego-1* by non-complementation with *ego-1/hT2* males and examination of DAPI stained individuals. Epistasis tests were done as follows. For *mpk-1*, we examined *ego-1(om58) unc-29;mpk-1(ga117)* and *ego-1(om97/+); mpk-1(ga117/+)* animals; *mpk-1* individuals were selected in the dissecting microscope on the basis of their vulval defective phenotype. For *ncc-1*, we examined *ego-1(om58) unc-29/++; ncc-1(he25ts) lon-1/++* animals raised either entirely at 20°C or at 15°C until young adulthood and then shifted to 20°C.

Molecular methods

Nucleic acids were isolated and manipulated using standard methods [32,36]. Probes were prepared using the Genius random primer kit (Boehringer). RNA blots were probed with *ego-1*-specific probes that did not cross-react with *ego-1*-related sequences on genomic DNA blots or cDNA screens. The loading control for RNA blots was *vit-2*, a yolk-protein gene that is transcribed in the intestine [37]. Partial cDNAs (yk42h7, yk288c2, yk406d11, yk349b2) were provided by Y. Kohara and colleagues. Other partial cDNAs were recovered by screening random-primed and poly(T)-primed libraries provided by R. Barstead. The cDNAs were restriction mapped, and a set of overlapping cDNAs was sequenced. Three cDNAs contained the poly(A) addition site and a portion of the poly(A) tail, but none appeared to contain the start codon. RT–PCR was used to recover the 5′ end. The RT reaction was done with wild-type total RNA and a primer located ~1 kb from the estimated 5′ end of the mRNA (AS8, 5′-GATAATGTGGGACGGAGTGCCG-3′) using the SuperScript Preamplification System (Gibco BRL). Primers in the PCR reaction were RTP14 (5′-ATGTCTGGATCGCCGCAATTAG-3′), located ~250 bp from the 5′ end, and SL1 (5′-GGTTTAATTACC-CAAGTTTGAG-3′), a *trans*-spliced leader sequence. Duplicates of the amplification product were cloned into the pGEM-T vector (Promega) and sequenced. Single-worm PCR was done essentially as described [33]. Product was either sequenced directly or first cloned into pGEM-T. In the former case, numerous PCRs were pooled; in the latter case, at least two independent clones were sequenced. Mutant changes were confirmed by sequencing additional clones and/or PCR products and by sequencing both strands. The parent strain, *unc-32(e189) glp 1(bn18ts)*, was sequenced as a control for background sequence changes that might not be associated with the *ego-1* phenotype. Proteins were aligned by the Clustal method. Expected values are a statistical measure of the likelihood that two sequences align by chance; an expected value of < 0.05 is considered significant.

RNAi

RNAi was done using a standard protocol [21]. Partial or complete cDNAs were linearized and transcribed in each direction, and complementary RNA products were annealed. We produced dsRNA from the *gld-1* plasmid, pLAJ1 [27], the *lag-1* plasmid, pGC2 (kindly provided by E.J. Hubbard), and the *ego-1* plasmid, pEL36 (this report). The *mpk-1* and *ncc-1* dsRNAs were kindly provided by A. Godbey and T. Schedl; *unc-22* dsRNA was kindly provided by A. Fire. The dsRNA was injected at a concentration of ~100–500 ng/μl. To test *ego-1* animals for susceptibility to RNAi, the following conditions were used. In *unc-22* tests, adults were injected; for other genes, young adults that had just molted to adulthood and/or L4 larvae were injected. When *unc-22* and *mpk-1* were tested together, L4 larvae were injected. For each gene, we determined when after injection a majority of control animals exhibited a mutant phenotype and then scored *ego-1* animals at this age. Conditions were as follows: *ncc-1*, *gld-1* and *mpk-1*, 2 days at 20°C; *lag-1*, 3 days at 20°C; *unc-22*, 4 days at 20°C; *unc-22* and *mpk-1* together, 3 days at 20°C. The *unc-22* phenotype was scored by observing whether animals twitched when paralyzed in 1.0 mM levamisole. Other phenotypes were scored in DAPI-stained animals. To test the *ego-1(RNAi); gld-2 gld-1* phenotype, *gld-2 gld-1 unc-29/hT2* adults were injected with pEL36 dsRNA; most of their F1 progeny were *ego-1*, but *unc-29* F1s were tumorous.

Supplementary material

Supplementary material including a sequence alignment of RRF proteins is available at http://current-biology.com/supmat/supmatin.htm.

Acknowledgements

We thank: Tim Schedl and Andy Fire for discussions, comments on the manuscript, and dsRNAs; Linda Ambrosio for comments on the manuscript; Karin Schneider for pGC2 and pEL36 dsRNA; Alan Coulson for cosmids; Stuart Kim, Tim Schedl and John Yochem for mutant strains; Robert Barstead for cDNA libraries; Yuji Kohara and colleagues for ESTs; Karen Bennett for *vit-2* plasmid; Doug Frank for advice on statistical tests. Many stocks were provided by the *Caenorhabditis elegans* Genetics Center, which is supported by the National Institutes of Health National Center for Research Resources. This work was supported by National Science Foundation funding (to E.M.M.).

References

1. Schedl T: **Developmental genetics of the germ line.** In *C. elegans II*. Edited by Riddle DL, Blumenthal T, Meyer BJ, Priess JR. New York: Cold Spring Harbor Laboratory Press; 1997, **5:**241-269.
2. Westlund B, Berry LW, Schedl T: **Regulation of germline proliferation in *Caenorhabditis elegans*.** *Adv Dev Biol* 1997, **5:**43-80.
3. Kimble J, Simpson P: **The LIN-12/Notch signaling pathway and its regulation.** *Annu Rev Cell Dev Biol* 1997, **13:**333-361.
4. Kuwabara P: **Developmental genetics of *Caenorhabditis elegans* sex determination.** *Curr Topics Dev Biol* 1999, **41:**99-132.
5. Francis R, Barton MK, Kimble J, Schedl T: ***gld-1*, a tumor suppressor gene required for oocyte development in *Caenorhabditis elegans*.** *Genetics* 1995, **139:**579-606.
6. Francis R, Maine E, Schedl T: **Analysis of the multiple roles of *gld-1* in germline development: interactions with the sex determination cascade and the *glp-1* signaling pathway.** *Genetics* 1995, **139:**607-630.
7. Kadyk LC, Kimble J: **Genetic regulation of entry into meiosis in *Caenorhabditis elegans*.** *Development* 1998, **125:**1803-1813.
8. Qiao L, Lissemore JL, Shu P, Smardon A, Gelber MB, Maine EM: **Enhancers of *glp-1*, a gene required for cell-signaling in *Caenorhabditis elegans*, define a set of genes required for germline development.** *Genetics* 1995, **141:**551-569.
9. Scheibel W, Pelissier T, Thalmeir S, Schiebel R, Kempe D, Lottspeich F, *et al.*: **Isolation of an RNA-directed RNA polymerase-specific cDNA clone from tomato.** *Plant Cell* 1998, **10:**2087-2102.
10. Cogoni C, Macino G: **Gene silencing in *Neurospora crassa* requires a protein homologous to RNA-dependent RNA polymerase.** *Nature* 1999, **399:**166-169.
11. Cogoni C, Macino G: **Isolation of *quelling-defective* (*qde*) mutants impaired in posttranscriptional transgene-induced gene silencing in *Neurospora crassa*.** *Proc Natl Acad Sci USA* 1997, **694:**10233-10238.
12. Wasseneger M, Pelissier T: **A model for RNA-mediated gene silencing in higher plants.** *Plant Mol Biol* 1998, **37:**349-362.
13. Fire A: **RNA-triggered gene silencing.** *Trends Genet* 1999, **15:**358-363.
14. Grant S: **Dissecting the mechanisms of posttranscriptional gene silencing: divide and conquer.** *Cell* 1999, **96:**303-306.
15. Sokal RR, Rohlf FJ: *Biometry*, Third Edition. New York: Freeman and Company; 1995.
16. Ellis R, Kimble J: **The *fog-3* gene and regulation of cell fate in the germ line of *Caenorhabditis elegans*.** *Genetics* 1995, **139:**561-577.
17. Graham PL, Kimble J: **The *mog-1* gene is required for the switch from spermatogenesis to oogenesis in *Caenorhabditis elegans*.** *Genetics* 1993, **133:**919-931.
18. The *C. elegans* Consortium: **Genome sequence of the nematode *C. elegans*: a platform for investigating biology.** *Science* 1998, **282:**2012-2018.
19. Aroian RV, Lesa GM, Koga M, Ohshima Y, Kramer JM, Sternberg PW: **Splicing in *Caenorhabditis elegans* does not require an AG at the 3′ splice site.** *Mol Cell Biol* 1993, **13:**626-637.
20. Beanan MJ, Strome S: **Characterization of a germ-line proliferation mutation in *C. elegans*.** *Development* 1992, **116:**755-766.
21. Fire A, Xu S, Montgomery MK, Kostas SA, Driver SE, Mello CC: **Potent and specific genetic interference by double-stranded RNA in *Caenorhabditis elegans*.** *Nature* 1998, **391:**806-811.
22. Lambie EJ, Kimble J: **Two homologous regulatory genes, *lin-12* and *glp-1*, have overlapping functions.** *Development* 1991, **112:**231-240.
23. Church DL, Guan K-L, Lambie EJ: **Three genes of the MAP kinase cascade, *mek-2, mpk-1/sur-1* and *let-60* ras, are required for meiotic cell cycle progression in *Caenorhabditis elegans*.** *Development* 1995, **121:**2525-2535.
24. Boxem M, Srinivasan DG, van den Heuvel S: **The *Caenorhabditis elegans* gene *ncc-1* encodes a *cdc2*-related kinase required for M phase in meiotic and mitotic cell divisions, but not for S phase.** *Development* 1999, **126:**2227-2239.
25. Kodoyianni V, Maine EM, Kimble J: **The molecular basis of loss-of-function mutations in the *glp-1* gene of *Caenorhabditis elegans*.** *Mol Biol Cell* 1992, **3:**1199-1213.
26. Jones AR, Francis R, Schedl T: **GLD-1, a cytoplasmic protein essential for oocyte differentiation, shows stage and sex-specific expression during *C. elegans* germline development.** *Dev Biol* 1996, **180:**165-183.
27. Petes TD, Malone RE, Symington LS: **Recombination in yeast**. In *The Molecular and Cellular Biology of the Yeast* Saccharomyces. Edited by Broach JR, Pringle JR, Jones EW. New York: Cold Spring Harbor Laboratory Press; 1993:407-521.
28. Scheibel W, Haass B, Marinkovic S, Klanner A, Sanger HL: **RNA-directed RNA polymerase from tomato leaves. II. Catalytic *in vitro* properties.** *J Biol Chem* 1993, **263:**11858-11867.
29. Guo S, Kemphues KJ: ***par-1*, a gene required for establishing polarity in *C. elegans* embryos, encodes a putative Ser/Thr kinase that is asymmetrically distributed.** *Cell* 1995, **81:**611-620.
30. Tabara H, Sarkissian M, Kelly WG, Fleenor J, Grishok A, Timmons L, *et al.*: **The *rde-1* gene, RNA interference, and transposon silencing in *C. elegans*.** *Cell* 1999, **99:**123-132.
31. Ketting RF, Haverkamp THA, van Luenen HGAM, Plasterk RHA: ***mut-7* of *C. elegans*, required for transposon silencing and RNA interference, is a homolog of Werner syndrome helicase and RNaseD.** *Cell* 1999, **99:**133-141.
32. Epstein HF, Shakes DC: Caenorhabditis elegans*: biological analysis of an organism*. Meth Cell Biol, vol 48. San Diego:Academic Press; 1995.
33. Hodgkin J: **Genetics.** In C. elegans *II*. Edited by Riddle DL, Blumenthal T, Meyer BJ, Priess JR. New York: Cold Spring Harbor Laboratory Press; 1997:881-1047.
34. McKim KS, Starr T, Rose AM: **Genetic and molecular analysis of the dpy-14 region in *Caenorhabditis elegans*.** *Mol Gen Genet* 1992, **233:**241-251.
35. Lackner MR, Kim SK: **Genetic analysis of the *Caenorhabditis elegans* MAP kinase gene *mpk-1*.** *Genetics* 1998, **150:**103-117.
36. Sambrook J, Fritsch EG, Maniatis T: *Molecular cloning: A Laboratory Manual*. New York: Cold Spring Harbor Laboratory Press; 1989.
37. Spieth J, Denison K, Kirkland S, Cane J, Blumenthal T: **The *C. elegans* vitellogenin genes: short sequence repeats in the promoter regions and homology to the vertebrate genes.** *Nucleic Acids Res* 1985, **13:**5283-5295.

Because *Current Biology* operates a 'Continuous Publication System' for Research Papers, this paper has been published on the internet before being printed. The paper can be accessed from http://biomednet.com/cbiology/cub – for further information, see the explanation on the contents page.